Solid State Sciences 13 (2011) 1205–1210

Contents lists available at ScienceDirect

Solid State Sciences

journal homepage: www.elsevier.com/locate/ssscie

Fabrication and characterization of an individual ZnO microwire-based UV photodetector

G.Y. Chai [a], L. Chow [a,b], O. Lupan [a,c,*], E. Rusu [d], G.I. Stratan [d], H. Heinrich [a,b], V.V. Ursaki [e], I.M. Tiginyanu [d,f]

[a] Department of Physics, University of Central Florida, PO Box 162385, Orlando, FL 32816-2385, USA
[b] Advanced Materials Processing and Analysis Center, and Department of Mechanical, Materials, and Aerospace Engineering, University of Central Florida, PO Box 162385, Orlando, FL 32816-2455, USA
[c] Department of Microelectronics and Semiconductor Devices, Technical University of Moldova, 168 Stefan cel Mare Blvd., MD-2004 Chisinau, Republic of Moldova
[d] Laboratory of Nanotechnology, Institute of Electronic Engineering and Industrial Technologies, Academy of Sciences of Moldova, MD-2028 Chisinau, Republic of Moldova
[e] Institute of Applied Physics of the Academy of Sciences of Moldova, MD-2028 Chisinau, Republic of Moldova
[f] National Center for Materials Study and Testing, Technical University of Moldova, MD-2004, Chisinau, Republic of Moldova

ARTICLE INFO

Article history:
Received 8 November 2009
Received in revised form
27 August 2010
Accepted 17 January 2011
Available online 26 January 2011

Keywords:
ZnO microwire
Photodetector
Ultraviolet UV
radiation

ABSTRACT

In this paper, a single ZnO microwire-based photodetector for the monitoring of ultraviolet (UV) radiation is described. Single crystal ZnO microwires were synthesized using a chemical vapor deposition (CVD) on the Si or Al_2O_3 substrate. The UV photodetector was fabricated by using in-situ lift-out method in a focused ion beam system to manipulate individual zinc oxide microwire. The photodetector prototype consists of a single ZnO microwire (20 μm in length) and exhibits a response of ~10 mA/W for UV light (365 nm) under 1 V bias. The transient response measurements revealed relatively fast response. The effect of oxygen adsorption and of different relative humidity conditions on the electronic transport through individual microwire is explored and discussed.

1. Introduction

In the past decade, ultraviolet rays reaching the earth's surface have intensified due to increasing stratospheric ozone depletion, and they may cause adverse effects on the human body, like high skin cancer rates, etc. In this connection there is a strong motivation for the development of small, low-cost, robust, and efficient ultraviolet (UV) detectors able to work in diverse conditions and that can be installed in different customer electronic devices easily. Besides this, UV photodetectors found wide applications in flame sensing, missile plume detection, chemical/biological analysis and advanced optical communications. For further developments a number of requirements and constrains like radiation hardness, reliability, light weight, minimal power consuming and order-of-magnitude performance advances in detectors and enabling technologies must be met.

II–VI semiconducting oxide materials have been regarded as promising materials due to their potential application in ultraviolet radiation detectors [1–10]. In this context, zinc oxide has been reported extensively for different UV detection applications [1–4], due to its radiation resilient properties [5,6], wide band gap of 3.36 eV that makes ZnO a strong candidate for high temperature electronic devices with reliable operation in space and other harsh environments. ZnO can emit laser light in the ultraviolet range up to room temperature, thus it can be used in highly-efficient miniaturized light sources (e.g. optical storage, microanalysis and in combination with a phosphor as bright white-light-source displays). Based on multiple advantages of ZnO for device applications in comparison with other wide band gap semiconductor materials, such as GaN, SiC, diamond, it is suitable for fabrication of long lifetime devices. Recent reports demonstrate fabrication of UV photodetectors using ZnO nano/microrods and wires [1–4].

To this date, ZnO materials have been grown by a variety of methods such as pulsed laser deposition, vapor phase transport process, chemical vapor deposition method, hydrothermal and aqueous solution deposition [1–12]. However, the nano-size makes

* Corresponding author. Department of Physics, University of Central Florida, PO Box 162385, Orlando, FL 32816-2385, USA. Tel.: +1 407 823 2333; fax: +1 407 823 5112.
E-mail addresses: guangyuchai@yahoo.com (G.Y. Chai), lupan@physics.ucf.edu (O. Lupan).

1293-2558/$ – see front matter © 2011 Elsevier Masson SAS. All rights reserved.
doi:10.1016/j.solidstatesciences.2011.01.010

the ZnO sensing devices not strong enough to survive under extreme environments or in consumer electronics. In order to develop reliable ZnO-based optical devices, the high quality zinc oxide structures with micrometer size are required to optimize the UV light sensing performance. Also, for UV photodetector applications, the presence of impurities in material will decrease the UV to visible rejection ratio. We employed chemical vapor deposition method to synthesize high quality ZnO microwires and employed photoluminescence and Raman spectroscopy to investigate their optical properties.

In this work, we demonstrate a method to fabricate single ZnO microwire-based UV detector and its characteristics under different relative humidity regimes that may lead to a next generation of micron size photodetectors for a wide area of applications.

2. Experimental

The growth of ZnO structures was carried out in a horizontal furnace with an argon/oxygen flow. A mixture of ZnO (99.99%) and graphite (99.999%) powders at molar ratio of 1:1 was used as source material. A temperature profile was set in the furnace with the maximum of 1030 °C at the place of the source material and 1000 °C at the Si or Al_2O_3 substrate. The growth process was performed in 1–2 h.

The morphology of the products was analyzed using a VEGA TS 5130MM scanning electron microscope (SEM) equipped with Energy Dispersion X-ray Spectrometer (EDX). Transmission electron microscopy (TEM) was performed with a FEI Tecnai F-30 microscope operating at 300 kV. The continuous wave PL was excited by the 351.1 nm line of a SpectraPhysics Ar^+ laser and analyzed with a double spectrometer ensuring the spectral resolution better than 0.5 meV. The samples were mounted on the cold station of a LTS-22-C-330 optical cryogenic system. The Raman scattering (RS) measurements were carried out at room temperature with a MonoVista CRS Confocal Laser Raman System in the backscattering geometry under the excitation by a 532 nm DPSS laser. An in-situ lift-out technique was used for the photodetector fabrication in a focused ion beam (FIB) instrument. The UV sensitivity was measured using a two-terminal ZnO microwire device. Current–voltage (I–V) characteristics were measured using a semiconductor parameter analyzer with input impedance of 2.00×10^8 Ω [1–3]. The fabricated single ZnO microwire-based photodetector was put in a test chamber to detect ultraviolet light. The readings were taken after a UV light was turned on. The UV source is an Hg-lamp with an incident peak wavelength of 365 nm and power output of 0.1 mW with online conductivity monitoring in ambient air.

3. Results and discussion

3.1. Structural characteristics

Fig. 1 shows a SEM micrograph of ZnO microwires. The average length and diameter of these ZnO microwires are 20–200 μm and 1–3 μm, respectively. It was also found that the cross-section of the ZnO microwires are well-defined hexagons, reflecting the wurtzite structure of ZnO. The energy dispersion X-ray spectroscopy (EDX) analysis of the produced structures demonstrates a stoichiometric ZnO composition. We found that the Zn:O ratios in our nanostructures correspond to 1:1 atomic ratio in all samples within the limits of the sensitivity of the EDX system of around 0.1 at.% (Fig. 1b). However, one should note that deviation from stoichiometry at the level of 0.1 at.% could generate a large amount of defects which seriously affect the electrical parameters of the material.

High resolution transmission electron microscopy (HRTEM) was employed to characterize the as-grown ZnO microwires. To prepare TEM samples, some of the ZnO microwire crystals were mechanically broken to generate atomic sharp edges for TEM examination. Fig. 2 shows the HRTEM images taken from one broken edge of the ZnO microwires. It can be observed that the ZnO crystal lattice is well oriented and no defects were evidenced in the examined region. The lattice spacing of 0.52 nm was calculated from the TEM image. The selected-area electron diffraction (SAED) pattern of the ZnO microwire materials are shown in the insert of Fig. 2. According to the SAED results, the microwire is grown along [0001] direction of ZnO, which corresponds to the HRTEM result.

3.2. Optical studies of ZnO microwires: PL and Raman

Fig. 3 shows the PL spectrum at 10 K from a ZnO microwire sample synthesized with CVD technique. It is dominated by the emission related to the recombination of donor bound excitons (D^0X) with I_4, I_8, and I_9 lines [12–14] and free excitons (FX). The D^0X emission is accompanied by LO phonon replica. The I_4, I_8, and I_9 lines are related to H, Ga, and In residual impurities with donor binding energy of 46, 55, and 63 meV, respectively [12]. These

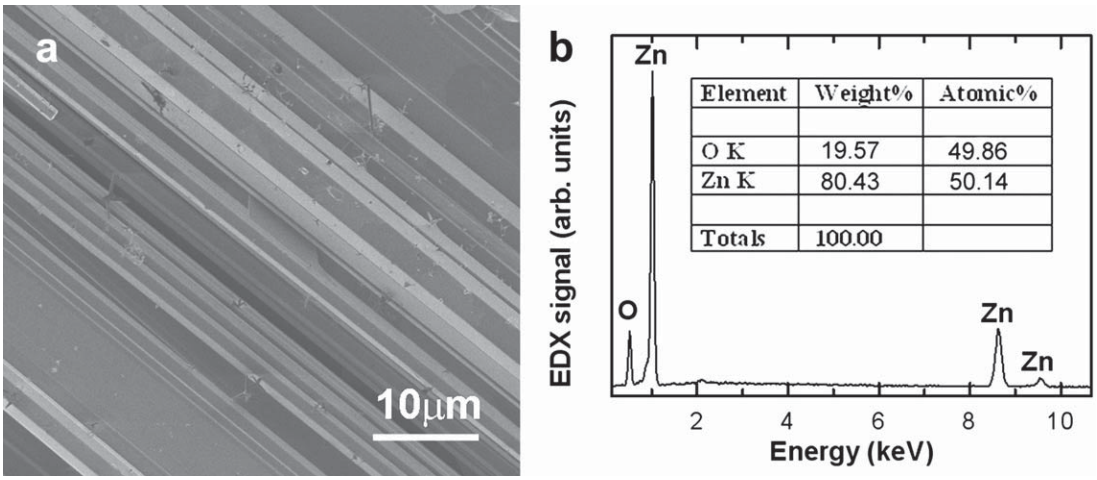

Fig. 1. SEM image of the CVD synthesized ZnO microwires (a) and the EDX analysis of the ZnO wire (b).

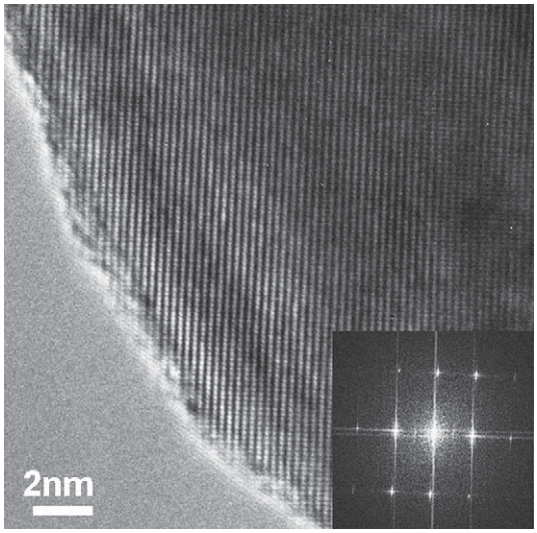

Fig. 2. TEM image taken from a side edge of CVD synthesized ZnO microwire and the insert shows a typical SAED pattern.

impurities, along with native defects such as zinc interstitial, determine the *n*-type conductivity of the material.

The Raman spectrum (RS) of ZnO structures is illustrated in Fig. 4. This spectrum demonstrates the good quality of the wurtzite crystal structure in the produced microwires. Wurtzite ZnO belongs to the C_{6v} space group ($P6_3mc$). According to group theory, the corresponding zone center optical phonons are $A_1 + 2B_1 + E_1 + 2E_2$ [15]. The $A_1 + E_1 + 2E_2$ modes are Raman active, while $2B_1$ are silent. The low-frequency E_2 mode is predominantly associated with the non-polar vibration of the heavier Zn sublattice, while the high frequency E_2 mode involves predominantly the lighter oxygen atoms. The A_1 and E_1 mode are split into LO and TO components. Except for the LO modes, all Raman active phonon modes are clearly identified in the measured spectrum (Fig. 4). The LO modes are not visible in the spectrum, likely due to the presence of a high free carrier concentration in the sample [11]. The peak at 331 cm^{-1}

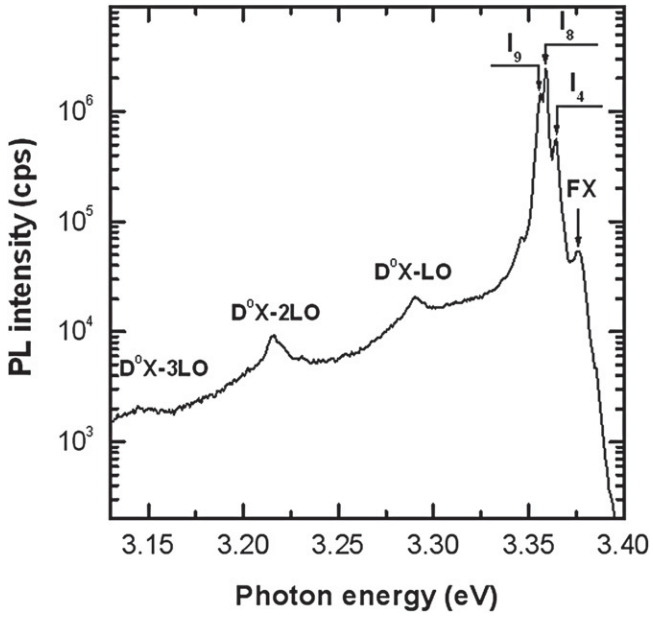

Fig. 3. PL spectrum of the ZnO microwire sample measured at $T = 10$ K.

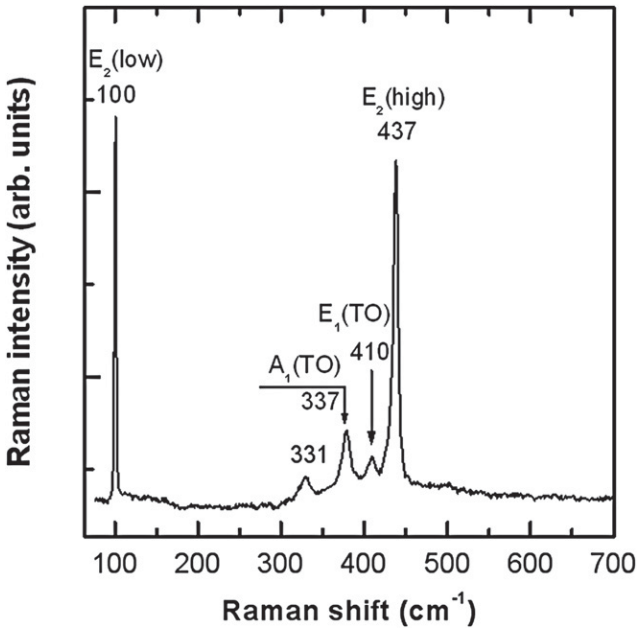

Fig. 4. Raman spectrum of a ZnO wire measured at room temperature.

is attributed to second order Raman processes involving acoustic phonons [16]. There are several indicators for a good crystal quality of the produced micro/nanostructures: (i) the signal attributed to the two-phonon density of states (DOS) expected in the spectral range from 500 to 700 cm^{-1} [17,18] is practically absent; (ii) the position of the E_2(high) peak corresponds to the one of bulk ZnO crystals [19] indicating a strain-free state of the micro/nanostructure; (iii) the peak corresponding to E_2(high) mode has a linewidth of about 6 cm^{-1}, while the linewidth of the peak corresponding to E_2(low) mode is about 2 cm^{-1}. The linewidth of 6 cm^{-1} of the E_2(high) mode is comparable to the values reported for high quality ZnO bulk crystals [20] and is supposed to be related to an intrinsic broadening. We suppose that this Raman scattering line is not affected by defects and impurities, in contrast to impurity effects observed recently in Mn doped ZnO semiconductors [22]. Moreover, the linewidth of 2 cm^{-1} of the E_2(low) mode is certainly not affected by defects, and is an indicator of a good crystal quality of the material.

3.3. Fabrication of photodetector by in-situ lift-out technique

Fig. 5a displays a top-view SEM image of ZnO microwires transferred to a Si/SiO_2 substrate. The in-situ lift-out technique was applied to fabricate the ZnO microwire photodetector [21]. The process was carried out in an FIB chamber equipped with a micromanipulator. The micromanipulator permits the spatial resolution of a 1–2 nm along *z* direction and about 5–10 nm for the *x* and *y* directions. The ZnO microwire samples were first transferred onto the intermediate Si/SiO_2 substrate in order to reduce the sample density and avoid electrical charging problems in the FIB system. Then low magnification was used to locate a target ZnO microwire with about 50 microns in length and 2 microns in diameter on the intermediate substrate. The FIB sample stage can be rotated and tilted to align the ZnO microwire to the desired direction. Afterward, an electro-etched tungsten needle mounted on the micromanipulator was lowered and brought into the FIB focus to approach the ZnO microwire sample. Once the needle touched the microwire, ion beam assisted Pt deposition was used to attach the

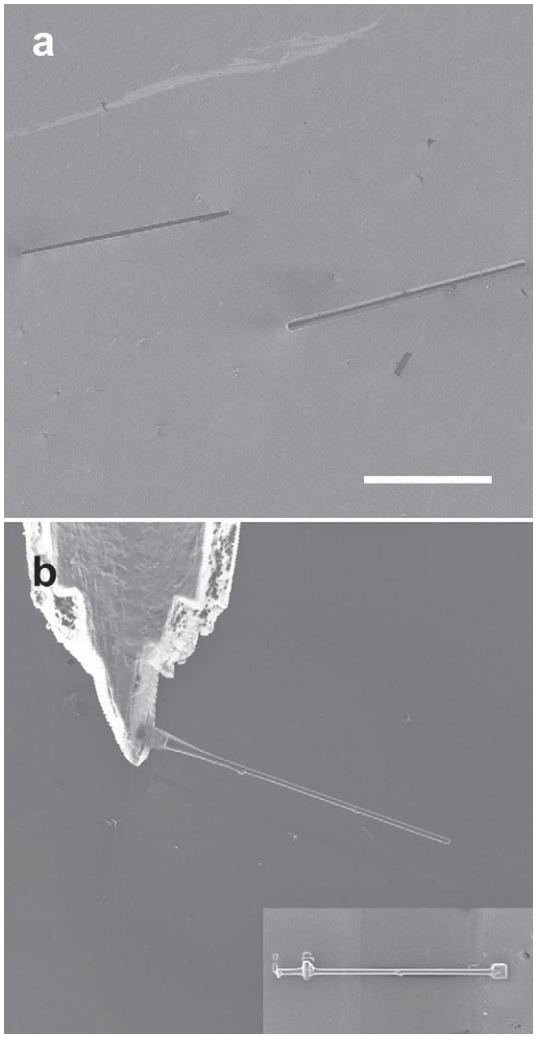

Fig. 5. In-situ lift-out fabrication of the single ZnO microwire UV photodetector. The scale bar is 20 μm.

microwire onto the W needle (Fig. 5b). Following this step the needle and specimen was raised away from the substrate. For the photodetector preparation, a glass substrate was used and Au/Ti electrodes were sputter deposited as template with external electrodes/connections. The gap between the electrodes was about 20 micron. With the help of the micromanipulator, the picked up ZnO microwire was placed right across the substrate electrode gap. Following that, the Pt deposition was used to mechanically and electrically attach both ends of the ZnO microwire to the Au electrodes. In the final step, the microwire was cut from the anchor point (end of the W needle) and the needle was raised away from the substrate. Fig. 5c shows the fabricated single ZnO microwire-based photodetector. The typical time to perform this in-situ lift-out FIB fabrication is about 20–30 min.

3.4. UV sensing properties

We studied the current–voltage (I–V) curves of the ZnO microwire with contacts realized by the in-situ lift-out method. Fig. 6 shows the dark characteristics of a single ZnO microwire-based photodetector in ambient air. The I–V measurements were performed by changing the bias voltages from +1 V to −1 V and vice versa. The voltage increment and delay time were set to 50 mV and 2 s. The curve in Fig. 6 is nearly linear, indicating good

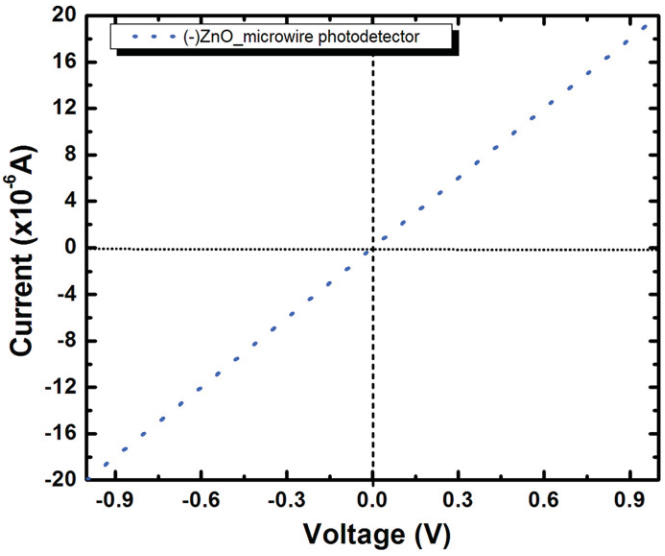

Fig. 6. I–V characteristic of the single ZnO microwire photodetector in the dark.

connection of the ZnO microwire with external electrical contacts and the ohmic contact nature.

The room temperature sensitivity of the single ZnO microwire photodetector to UV light is shown in Fig. 7. The device was subjected to irradiation with 365 nm UV light in ambient air with electrical resistance monitoring. The UV radiation is applied perpendicular to the substrate surface. The background atmosphere was ambient air with relative humidity (RH) of 53%.

According to the results presented in Fig. 7 when the UV light is turned on, the electrical resistance ratio decreases about 1.2%. Afterward, when the UV light is turned off, the detector resistance increases back to the initial value. The UV sensing phenomenon can be explained by the variation of the electrical charge carrier density. As-grown ZnO microwires absorb O_2 molecules on the surface:

$$O_2(g) + e^- \rightarrow O_2^-(ad), \quad \frac{1}{2}O_2(g) + e^- \rightarrow O^-(ad), \quad \frac{1}{2}O_2(g) + 2e^- \rightarrow O^{2-}(ad) \tag{1}$$

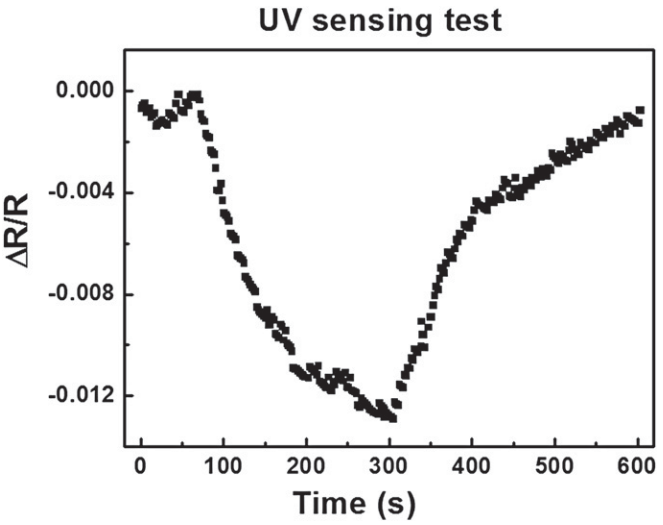

Fig. 7. UV sensitivity measurement of the fabricated single ZnO microwire device structure.

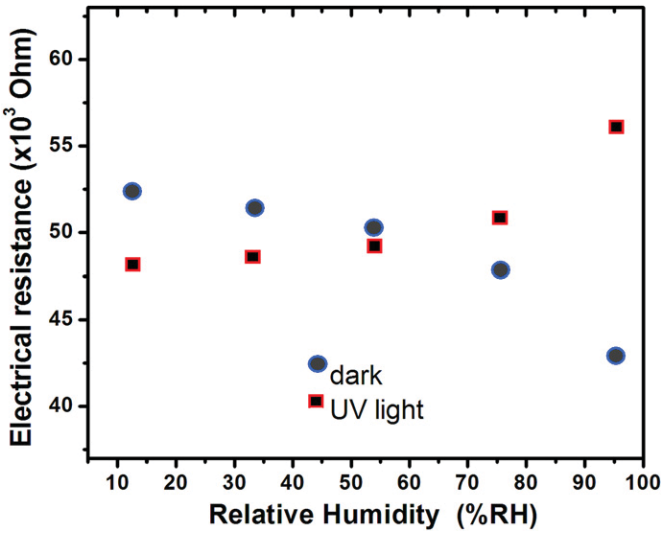

Fig. 8. Dependence of the electrical resistance of single ZnO microwire device structure versus relative humidity in the dark and under UV light.

they will take free electrons from the *n*-type ZnO materials, which results in decreasing of the carrier density and of their mobility. As a result a depletion region is formed. After turning on the UV light, electron–hole pairs will be generated to increase the charge carrier density which results in the reduction of the ZnO microwire resistance. When the electron–hole pairs are generated, the holes will migrate to the surface and recombine with previously adsorbed and ionized oxygen ions and annihilate the depletion region. At the same time the exceed electrons will contribute to the increase of the conductivity. The UV response time determined by the e^--h^+ generation and recombination rates is in the order of 50–75 s. The slow rise time is thought to be determined by surface effects such as oxygen adsorption and desorption. The decay time follows a fast and a slow process which relate to the recombination of photo-generated e^--h^+ pairs (solid-state process) and O_2 readsorption (surface effects), respectively. This proves to be comparable with the response time of our previously fabricated ZnO – based UV photodetector [1,2]. Several photodetectors have been fabricated by the same in-situ lift-out technique and have been investigated under identical conditions. Similar UV responses were observed. Therefore, with an energy band gap of 3.31 eV at room temperature, zinc oxide microwires are promising candidate for "visible-blind" photodetection.

Next we explored the UV photoresponse of ZnO microwire under different relative humidity conditions. Relative humidity (RH) measurements were realized using a saturated salt solution method described elsewhere [23]. Fig. 8 presents the variation of the electrical resistance of ZnO microwire-based detector in the dark and under UV illumination for different RH values. The electrical resistance of device structure in the dark decreases with the increase of the relative humidity from 12 to 97%. We propose the following sensing mechanism. It is considered that the variation of the resistance value with humidity is due to the adsorption of water molecules on the surface of the zinc oxide microwire. The water vapors are adsorbed at the surface in molecular or hydroxyl forms and reversibly react with the Zn sublattice and donate electrons as follows:

$$H_2O + O_O + 2Zn_{Zn} \leftrightarrow 2(OH - Zn) + V^{\cdot\cdot} + 2e^- \quad (2)$$

where O_O is the oxygen in the lattice site, and $V^{\cdot\cdot}$ is the vacancy created at this site and ionized. According to equation (2) the resistance decreases with the relative humidity increase due to the formation of free electrons. It was suggested that water molecules replace the previously adsorbed and ionized oxygen (O^-, O^{2-}, etc.) and therefore release the electrons from the ionized oxygen [23]. Probably the "donor effect" could result from both.

On the other hand, the device structures under UV illumination exhibit a higher electrical resistance for RH>53%, which implies a lower reactivity of Zn with the water vapors. The water molecules rapidly occupy the available sites upon atmospheric exposure. While the first layer of chemi-adsorbed water is formed at low relative humidity, the next layers of water molecules are physically adsorbed.

The adsorbed water in the chemi-adsorbed layer dissociates due to strong electrostatic fields according to the equation:

$$2H_2O \leftrightarrow H_3O^+ + OH^- \text{ or } H_2O \leftrightarrow H^+ + OH^- \quad (3)$$

The charge transport occurs according to the Grotthuss reaction when H_3O^+ release a proton which is accepted by the neighboring water molecule, therefore releasing another proton. At relative humidity exceeding 40%, the adsorbed water is condensed on surface which results in electrolytic conductivity in addition to the proton conductivity [24].

Because the conductivity is caused by the surface concentration of electrons, this sensing style is usually called "electronic type". However, the water layer formed by the physical adsorption may be somewhat proton-conductive. Therefore, at room temperature the conductivity of ceramic semiconducting materials is actually due to addition of both electrons and protons (ionic), unless at high temperatures (>100 °C) moisture cannot effectively condense on the surface [23].

Under UV light the electron–hole pairs are generated and affect electrical current (respective resistance) value. However the dissociated water molecules on the surface may extract electrons and holes at the same time and contribute to creation of a depletion region and increase of resistance, especially under high RH. Thus, the number of electrons and holes are comparable and when UV light is turned off they will recombine quicker and lead to a faster decay. In our experiments it was observed a smaller decay time for tests in ambient with RH > 53% which makes more promise and faster response device to be used in a humid ambient. It can be explained by the less bended energy bands near to the ZnO surface due to the lower quantity of O_2^- ions adsorbed. Thus, electrons and holes can recombine faster reducing the time decay after switching off UV light. However, at the same time we observed a humidity-induced degradation of ZnO-based photodetector structure at relatively high RH values. It could be due to the diffusion and reaction of mobile H^+ proton generated by dissociation of water as shown in Eq. (3) at the surface of microwire. H^+ proton are very reactive and can diffuse [25], which lead to degradation in time. These results suggest the idea to use some protective layers on ZnO microwire-based photodetector. More details about the impact of humidity on ZnO – based photodetectors will be presented in a forthcoming paper.

4. Conclusions

In this work, a single ZnO microwire photodetector for the monitoring of ultraviolet radiation is successfully demonstrated. The ZnO microwire materials were synthesized with CVD method. The SEM, TEM, Raman, and photoluminescence results show the high quality of the ZnO single crystal material. FIB in-situ lift-out technique is applied to fabricate the single ZnO microwire UV detector. It shows reliable UV sensitivity and high promise of ZnO microwire as an active material for UV device applications. The electrical resistance of the structure in the dark decreases with the

relative humidity value. Besides, under UV light expose it was observed an increase in R value for higher RH. These single ZnO microwire UV detecting devices are expected to find major applications in space and other harsh environments.

Acknowledgments

L. Chow acknowledges partial financial support from US Department of Agriculture award #58-3148-8-175. Financial support by the Supreme Council for Science and Technological Development of the Academy of Sciences of Moldova (Project 036/R) are gratefully acknowledged. Dr. Lupan acknowledges support for researcher position in Professor Chow's group.

References

[1] O. Lupan, L. Chow, G. Chai, L. Chernyak, O. Lopatiuk-Tirpak, H. Heinrich, Phys. Status Solidi A 205 (2008) 2673.
[2] G. Chai, O. Lupan, L. Chow, H. Heinrich, Sensors Actuators A: Phys. 150 (2009) 184.
[3] O. Lupan, G. Chai, L. Chow, Sensors Actuators B. Chem. 141 (2009) 511.
[4] Y. Li, F.D. Valle, M. Simonnet, I. Yamada, J.-J. Delaunay, Nanotechnology 20 (2009) 045501.
[5] R.E. Peale, E.S. Flitsiyan, C. Swartz, O. Lupan, L. Chernyak, L. Chow, W.G. Vernetson, Z. Dashevsky, Neutron transmutation doping and radiation hardness for solution-grown bulk and nano-structured ZnO (Mater. Res. Soc. Symp. Proc. Volume 1108, Warrendale, PA, 2009). in: M. Mastro, J. LaRoche, F. Ren, J.-I. Chyi, J. Kim (Eds.), Performance and Reliability of Semiconductor Devices, vol. 1108. Materials Research Society Symposium Proceedings, 2009, pp. 55–60.
[6] (a) A. Burlacu, V.V. Ursaki, V.A. Skuratov, D. Lincot, T. Pauporte, H. Elbelghiti, E. Rusu, I.M. Tiginyanu, Nanotechnology 19 (2008) 215714; (b) D.C. Look, D.C. Reynolds, J.W. Hemsky, R.L. Jones, J.R. Sizelove, Appl. Phys. Lett. 75 (1999) 811.
[7] H. Kind, H. Yan, B. Messer, M. Law, P. Yang, Adv. Mater. 14 (2002) 158.
[8] Z. Fan, P.-C. Chang, J.G. Lu, E.C. Walter, R.M. Penner, C.-H. Lin, H.P. Lee, Appl. Phys. Lett. 85 (2004) 6128.
[9] O. Lupan, L. Chow, G. Chai, B. Roldan, A. Naitabdi, A. Schulte, H. Heinrich, Mat. Sci. Eng. B 145 (2007) 57.
[10] L. Chow, O. Lupan, H. Heinrich, G. Chai, Appl. Phys. Lett. 94 (2009) 163105.
[11] V.V. Ursaki, E.V. Rusu, A. Sarua, M. Kuball, G.I. Stratan, A. Burlacu, I.M. Tiginyanu, Nanotechnology 18 (2007) 215705.
[12] B.K. Meyer, H. Alves, D.M. Hofmann, W. Kriegseis, D. Forster, F. Bertram, J. Christen, A. Hoffmann, M. Strassburg, M. Qworzak, U. Haboeck, A.V. Rodina, Phys. Stat. Sol. (b) 241 (2004) 231.
[13] V.V. Ursaki, I.M. Tiginyanu, V.V. Zalamai, E.V. Rusu, G.A. Emelchenko, V.M. Masalov, E.N. Samarov, Phys. Rev. B. 70 (2004) 155204.
[14] J. Petersen, C. Brimont, M. Gallart, O. Cregut, G. Schmerber, P. Gilliot, B. Hönerlage, C. Ulhaq-Bouillet, J.L. Rehspringer, C. Leuvrey, S. Colis, H. Aubriet, C. Becker, D. Ruch, A. Slaoui, A. Dinia, J. Appl. Phys. 104 (2008) 113539.
[15] A. Kaschner, U. Haboeck, M. Strassburg, G. Kaczmarzyk, A. Hoffmann, C. Thomsen, A. Zeuner, H.R. Alves, D.M. Hofmann, B.K. Meyer, Appl. Phys. Lett. 80 (2002) 1909.
[16] M. Rajalakshmi, A.K. Arora, B.S. Bendre, S. Mahamuni, J. Appl. Phys. 87 (2000) 2445.
[17] F. Reuss, C. Kichner, Th. Gruber, R. Kling, S. Maschek, W. Limmer, A. Waag, P. Ziemann, J. Appl. Phys. 95 (2004) 3385.
[18] J. Serrano, A.H. Romero, F.J. Manjon, R. Lauck, M. Cardona, A. Rubio, Phys. Rev. B. 69 (2004) 094306.
[19] J. Serrano, F.G. Manjon, A.H. Romero, F. Widulle, R. Lauck, M. Cardona, Phys. Rev. Lett. 90 (2003) 055510.
[20] O. Lupan, T. Pauporté, L. Chow, B. Viana, F. Pellé, B. Roldan Cuenya, L.K. Ono, H. Heinrich, Appl. Surf. Sci. 256 (2010) 1895.
[21] O. Lupan, G. Chai, L. Chow, Microelectron. J. 38 (2007) 1211.
[22] J. Alaria, M. Bouloudenine, G. Schmerber, S. Colis, A. Dinia, J. Appl. Phys. 99 (2006) 08M118.
[23] Z. Chen, C. Lu, Sensor Lett. 3 (2005) 274.
[24] B.M. Kulwicki, J. Am. Ceram. Soc. 74 (1991) 697.
[25] M.-H. Wang, K.-A. Hu, B.-Y. Zhao, N.-F. Zhang, Ceram. Int. 33 (2007) 151–154.